Heat and Mass Transfer 33 (1997) 27–39 © Springer-Verlag 1997

Thermochromic liquid crystals and true colour image processing in heat transfer and fluid-flow research

J. Stasiek

Abstract In the last five years or so, true-colour image processing has gone being available mainly to highly technical users on expensive image processing systems to being used by virtually anyone who can use a desktop computer. Also, during the past 25 years, liquid crystals have emerged as reliable temperature sensors for heat transfer research, and have been applied in a number of situations to visualise the temperature distribution under complex flow fields. In this study the true-colour image processing of the liquid crystal (LC) images was developed successfully and applied to the study of heat and mass transfer problems. The history of this technique is reviewed and principal methods are described and some examples are presented.

1
Introduction

Liquid crystals are highly anisotropic fluids that exist between the boundaries of the solid phase, and the conventional, isotropic liquid phase. Some liquid crystals materials (cholesteric or chiral nematic type) can exhibit scientifically valuable colour effects with a visible spectrum when they are heated to specific temperature ranges. Since the colour change is reversible and repeatable, they can be calibrated accurately with proper care and used in this way as temperature indicators. They can be painted on a surface or suspended in a fluid and used to indicate visibly the temperature distribution. In this way, liquid crystals have been successfully applied to heat transfer and fluid flow research.

During the past ten years there has been an increasing use of digital image processing in heat transfer and fluid flow laboratories, first to facilitate conventional experiments and then to expand the range of possible work. In the early days of image processing, monochrome systems were the only ones available. Soon after the colour image processing became more accessible monochrome systems continued to dominate because they were easier and less costly.

Nowadays colour image processing has become an integral part of many scientific and industrial applications. A great majority of applications that use colour image processing do so because colour is the most important and obvious feature of the images they are examining.

These new tools (liquid crystals, computers and image processing) have come together during the past few years to produce a powerful new examination technique: true-colour digital processing of liquid crystal images to yield full-field temperature, velocity and heat transfer coefficient distributions. Now, new and more incisive experiments are being used in conventional situations, while those which have been previously intractable can also be studied.

In this paper we carefully review the above issues, and use illustrative examples from our own work in applying TLC to the study of forced and natural convective heat transfer, on a cooled surface heated by air flow disturbed by a number of complex geometrical configurations, and for temperature and flow visualisation in a rectangular cavity respectively.

2
Liquid crystals

Liquid crystals constitute a class of matter unique in exhibiting mechanical properties of liquids (fluidity and surface tension) and optical properties of solids (anisotropy to light, birefringence). Although they were first observed more than 100 years ago by an Austrian botanist, Friedrich Reinitzer, studies of liquid crystals were confined to material laboratories until the 60's when applications to science and engineering began [8] [16].

Liquid crystals are temperature indicators that modify incident white light and display colour whose wavelength is proportional to temperature. They can be painted on a surface or suspended in the fluid and used to make visible the distribution of temperature. Normally clear, or slightly milky in appearance, liquid crystals change in appearance over a narrow range of temperature called the "colour-play interval" (the temperature interval between first red and last blue reflection), centred around the nominal "event temperature". The displayed colour is red at the low tem-

Received on 20 September 1996

Prof. Dr. Jan Stasiek
Technical University of Gdańsk
Faculty of Mechanical Engineering
Narntowicza 11/12, 80-952, Gdańsk, Poland

This paper is an extension of a presentation as an invited lecturer at the EUROMECH COLLOQUIUM 335 on Image Techniques in Fluid Dynamics, University of Rome, "La Sapienza", Engineering Faculty, 5–7 June, Rome, 1995. Also I am very grateful to Prof. A. Cenedese and Dr. G.P. Romano for their attentive support and conducive atmosphere during my stay in Rome.

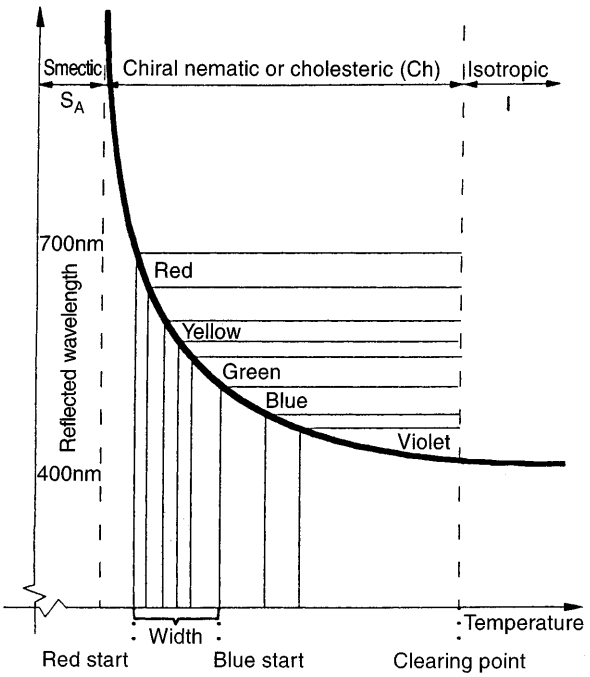

Fig. 1. Typical reflected wavelength (colour) temperature response of a temperature-sensitive liquid crystal mixture

perature margin of the colour-play interval and blue at the high end. Within the colour-play interval, the colours change smoothly from red to blue as a function of temperature [14]. The effect (illustrated in Fig. 1) is reversible which, in practical terms, means that a single application of liquid crystals to a model can be used repeatedly (usually until the coating is oblated or otherwise damaged).

Both the colour play interval and the event temperature range of a liquid crystal can be selected by adjusting its composition, and materials are available with event temperatures from −30°C to 120°C and with colour play bands from 0.5°C to 20°C, Jones et al. [12] and Moffat [14], although not all combinations exist of event temperature and colour play band widths. Widths of 1°C or less will be called narrow band materials, while those whose band width exceeds 5°C will be called wide-band. The types of material to be specified for a given task depend on the type of image interpretation technique to be used.

Liquid crystals are classified into three categories according to their molecular structures: smectic; nematic, and cholesteric. However, from a structural viewpoint, it

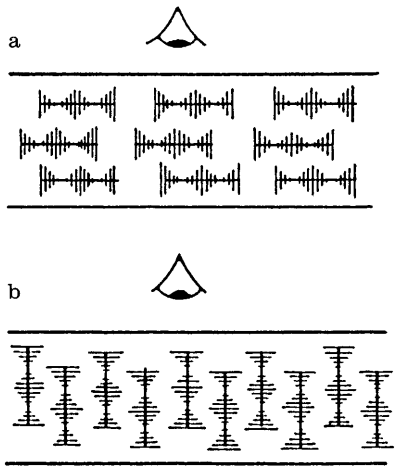

Fig. 3a,b. Orientations of helical (long lines) and molecular axis (short lines) relative to observer **a** Focal conic texture and **b** Grandjean or Planar texture

can be argued that there are only two basic types of liquid crystal; chiral-nematic and smectic, with cholesteric being regarded as a special kind of nematic. Their structures are shown schematically in Fig. 2. A question of great relevance is the texture taken up by the cholesteric phase which can exhibit two forms; the focal-conic and the grandjean textures Fig. 3. In the focal-conic texture the cholesteric helices pack around elliptical and hyperbolic paths whereas in the grandjean form the helical axes are in the same direction and large regions of aligned molecules are present. This texture is birefringent but optically inactive. In the grandjean texture, which forms from the focal-conic by mechanical shear, the helices are more or less all aligned with their axis parallel to incident light. This is the texture that exhibits the unique optical effects of the mesophase-iridescence, optical activity, circular dichroism and selective reflection of white light to show brilliant colour [15].

Pure liquid crystal materials are thick, viscous liquids, greasy and difficult to deal with under most heat transfer laboratory conditions [14]. Two approaches have been used to make them more practical to use:

(i) encapsulation of the liquid crystal in a gelatine-like material forming nearly spherical particles from 10-30 microns in diameter and then making a paint using those particles as the pigment, or

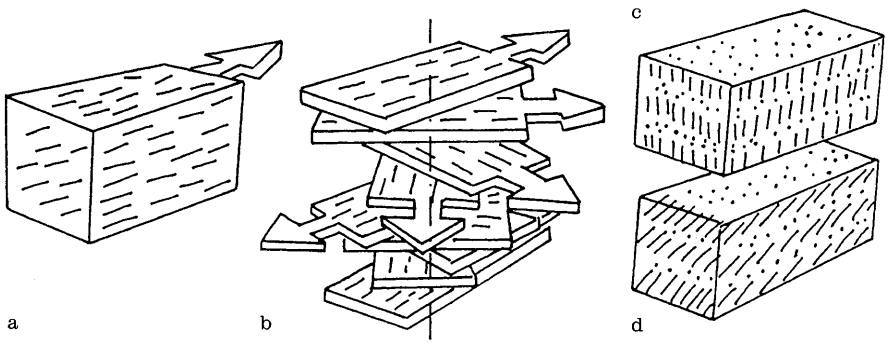

Fig. 2a–d. A different view of the mesophase structure. The orientation of the molecular director is represented by the arrows: **a** Nemataic, **b** Cholesteric, **c** Smectic A and **d** Smectic B. (Jones et al. [12] and MERC Ltd. [25])

(ii) application of the unencapsulated material (unsealed liquids) to a clear plastic sheet and sealing it with a black backing coat to form a pre-packaged assembly. This is because in their (pure) exposed state TLC quickly degrade.

The majority of commercial temperature indicating devices using TLC contain a thin film of the liquid crystal sandwiched between a transparent polyester sheet and a black absorbing background, however in the current experiment the liquid crystals are deposited on the black painted sheet. That is, liquid crystals layer in direct contact with the fluid (front print). Excellent papers on this aspect of liquid technology have been published by Brown and Shaw [6], Fergason [8], Stephan and Straley [20] and more recently by Jones et al. [12], Parsley [15] and the manufacturers' handbooks [25]. Also liquid crystals can be used to make visible the temperature and velocity fields in liquids by the simple expedient of directly mixing the liquid crystal material into the liquid, in very small quantities (0.01 to 0.03% by weight are recommended) [14] [15] [17]. The encapsulated form of both chiral-nematic and cholesteric liquid crystal can be mixed directly into water, glycerol, glycol and silicone oils to use thermal and hydrodynamic tracers. Any collimated source of white light can be used (laser illumination is not required) and quite good results have been obtained using a narrow slit projected through a conventional photo flash lamp or slide projector. In the present experiments for flow visualisation unencapsulated chiral-nematic material (type TM 256 from BDH Chemicals Limited) was used to determine both the temperature and velocity fields of natural convection flow within a rectangular enclosure.

3
True-colour image processing technique

In the early days of image processing, only monochrome systems were available. Soon after the colour image processing became available but monochrome systems continued to dominate because they were easier and less costly to manufacture and less complicated to use. There are several commercial packages of hardware and software available which can digitize a video image from either black and white or colour cameras and store individual frames pixel by pixel in arrays. Three separate arrays are used to store a colour image, one for the red, green and blue signal components. Also, three styles of camera have been used: NTSC composite (the usual home video camera), CCD (charge-coupled device) and CID (charge injected device). According to Akino et al. [1], Moffat [14] and Jones et al [12]. there are four broad classes of image interpretation techniques available: human observers, multiple narrow-band spectral intensity image processing system, multiple linear regression method and true-colour or chromaticity based image processing systems.

Human observers can interpret liquid crystal images by direct visual inspection of colour photographs or tape recorded video images, usually using narrow-band points. Calibrations for such use are generally limited to identifying the temperature associated with a particular colour often the red or the yellow-green colour near the centre of the colour-play band. The uncertainty associated with direct visual inspection is about 1/3 the colour-play bandwidth, given an observer with normal colour vision and a little experience, Moffat [14], or about $\pm 0.2^{\circ}$C to 0.5°C, depending on the band width. The second and third methods are based on the interferential optical filters with narrow band-play characteristics of transmittance, through which equally coloured regions can be extracted. Akino et al. [1] [2] developed a multiple narrow-band spectral intensity interpreter using a set of eighteen narrow band-pass filters, whose central wave-lengths were from 400 to 750 nm, and the full width of the half maximum (FWHM) of the filters were less than 10 nm. The behaviour of liquid crystals can be interpreted in terms of the variation of intensity with wavelength, at a given temperature instead of the variation of dominant Hue with temperature. When the temperature distribution on the specimen spans the colour-play-band-width of the liquid crystal, viewing that surface through any one filter will, in principle, display a line whose position indicates the location where that particular wavelength is most bright; an isotherm of known temperature after calibration. Good results were obtained, by these same authors (Akino et al. [1] [2]), using sets of three filters, chosen considering the spectral characteristics of the microencapsulated liquid crystals used in conjuction with the lighting. Temperature was expressed as a linear function of the intensities passed by the three filters (red, green and blue). With three filters, four coefficients are required, and those were found by calibration. The authors quote an uncertainty of $+/-0.1^{\circ}$C for the method and a spatial resolution of 1 mm. The spatial resolution was set by the lens used, and the face area of one pixel and is not a limitation on the method [1][2][14].

In the fourth method Hollingsworth et al. [11] approached the image interpretation problem from the standpoint of standard colour video practice, electing to work with the relationship between the dominate Hue and temperature as the primary function, rather than the intensity distribution as a function of wavelength. The relative functions of red, green and blue (RGB) determine perceived colour, and also can be treated as the independent variables with which to represent the colour numerically. In this method a displayed RGB image is immediately perceived by a user as exhibiting three distinct attributes (HSI): Hue – the spectral colours present, Saturation – how deep or faded the colour appears to be, and Intensity – the edge information or what would be seen if a black-and-white version of the image were displayed (hence, only intensity is available from a monochrome system).

The uncertainty of true-colour interpreters using wide-band liquid crystals is of the same order as the uncertainty resulting from human observers using narrow-band materials. It depends on the pixel-to-pixel uniformity of the applied paint and on the size of the area averaged by the interpreter [11] [14].

Many image processing operations developed for processing grey-level (intensity) images can be readily applied to HSI colour images. These include image transformations, enhancement, analysis, compression, transformation and restorations. Building on grey-scale image processing hardware and software, Data Translation has produced a 512 $\times$ 512 pixels $\times$ 8 bit per colour compo-

nent colour frame-grabber board for PC/ATs which takes up a 256 K byte of memory [24].

A schematic view of such an image processing system (developed by the author) is shown in Fig. 4. The two dimensional temperature distribution is determined using RGB video-camera, IBM 386 Personal Computer AT, HSI Colour Frame Grabber DT 2871 and Auxiliary Frame Processor DT 2858. As shown, the chart is also for an RGB video-recorder (JVC-S605E), includes a Time Based Corrector VT 3000 and KMV7EK RGB convertor. New chart with JVC-S605E as the terminal makes it possible for presentation tapes to be loaded, cued and played exactly on schedule with all operation handed by the computer. For fast and transit method, accurate location of specific scenes or edit points JVC-S605E is provided with a convenient, easy-to-use search dial. A time base corrector (TBC) controls times tracking systems and easy identification colour-coded images.

Before the execution of a thermal or flow visualisation experiment, we should recognise the characteristics of the overall combination of the TLC, the light source, the optical and camera system (ordinary, CCD black and white or RGB colour camera), and make a rational plan for the total measurement system. The relationship between the temperature of the crystal and the measured Hue of the reflected light defines the calibration curve for the liquid crystal. The result is a curve relating the Hue of the reflected light to the surface temperature. A known temperature distribution exists on a "calibration plate" (brass plate) to which is attached the liquid crystal layer. In order to maintain a linear temperature distribution with desired temperature gradients, one end of a brass plate was cooled by stabilised water and the other end controlled electrically to give a constant temperature [1] [17]. The brass plate with the liquid crystal layer is calibrated in place in the wind tunnel with the same lighting level and viewing angle used during the data acquisition phase of the experiment. The distribution of the colour component pattern on the liquid crystal layer was measured by RGB colour camera and a series of images at different temperatures defines the calibration. A representative calibration curve including Hue and temperature distribution along the plate is shown in Fig. 5 [18] [19].

The liquid crystals used here, manufactured in sheet form by B & H Limited (Fig. 6), had an event temperature range of 30.7–33.3°C. In the actual measurements, only the yellow-green colour band corresponding to $t_l = 32.1$°C was used as it is the brightest and sharpest. In this particular experiment uncertainty was estimated as about ±0.05°C by considering only the section of the surface used in the experiment, spanwise non-uniformities in Hue value are minimized.

4
Experimental technique

Two main methods of measurement are performed involving steady state and transient techniques. A brief history of these is given by Baughn et al. [4]. Recent reviews of heat transfer measurements have also been produced by Moffat [14], Jones et al. [12] and Ashforth-Frost et al. [3].

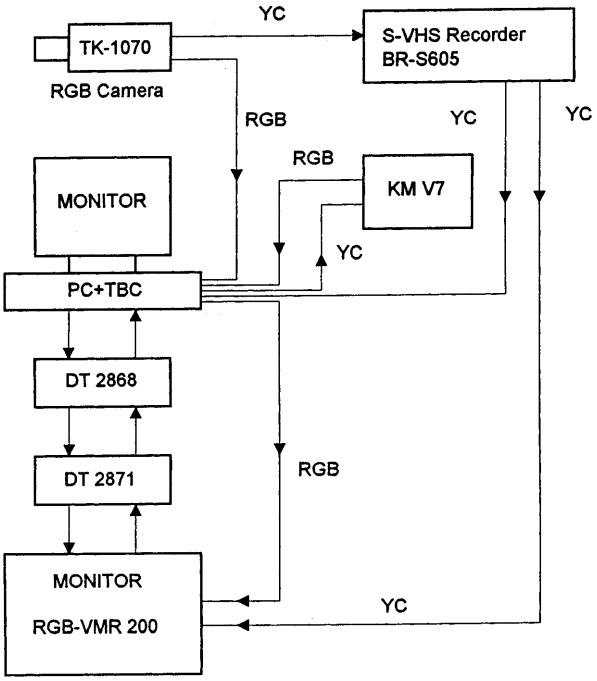

Fig. 4. The information flow chart for a true-colour image interpreter and computer-controlled video system

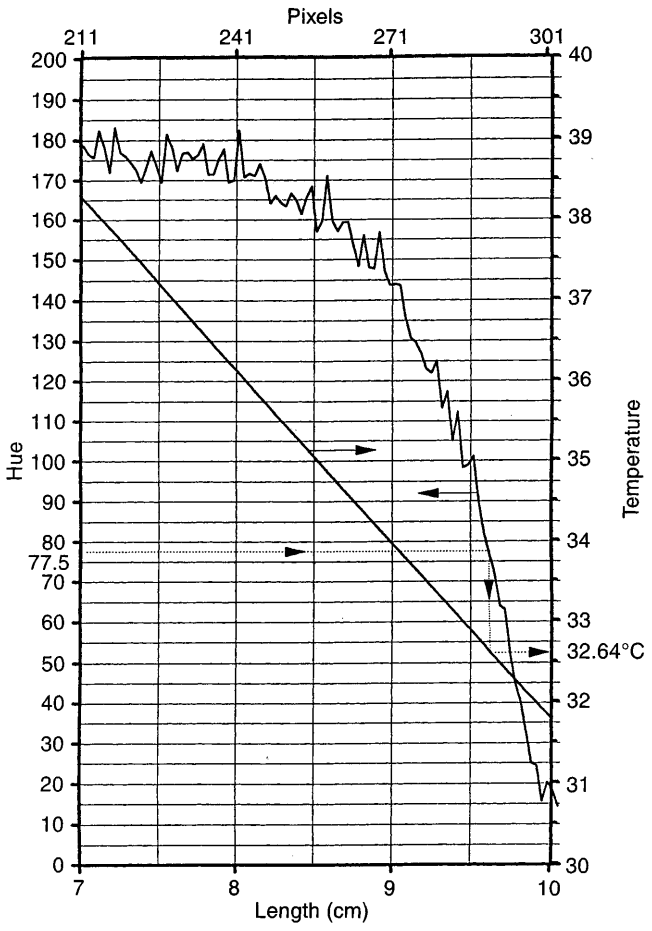

Fig. 5. Representative calibration curve – Hue and temperature distribution along the test plate

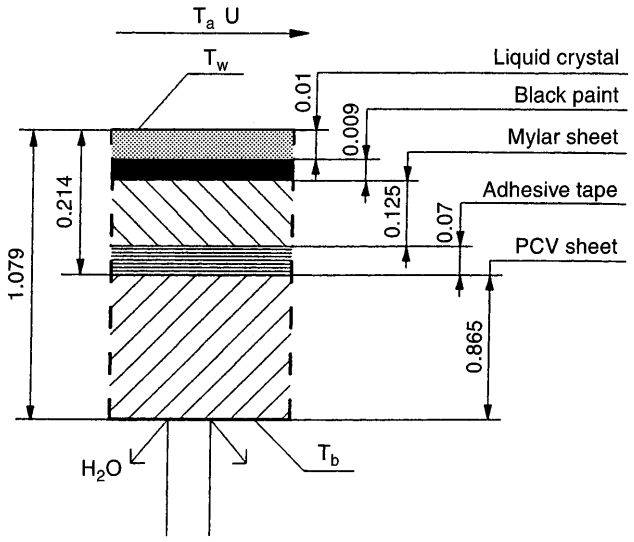

Fig. 6. Liquid crystal package (front print)

(a) Steady state analyses – constant flux method
The steady state techniques employ a heated model and the TLC is used to monitor the surface temperature. Usually, a surface electric heater is employed such that the local flux, q is known and this, together with the local surface temperature, T_w, (found from the TLC), gives the local heat transfer coefficient, h,

$$q = I^2 r \text{ and } h = \frac{q}{T_a - T_w} \tag{1}$$

T_a is a convenient driving gas temperature, I is the current and r is the electrical resistance per square of the heater.

(b) Steady state analyses – uniform temperature method
The TLC-coated test specimen forms one side of a constant temperature water bath and is exposed to a cool/hot air flow. The resulting thermograph is recorded on film or video and further measurement positions are obtained by adjusting the water bath temperature. This method is more time consuming due to the large volume of water that needs to be heated. In this case, the heat transfer coefficient is determined by equating convection to the conduction at the surface,

$$h(T_a - T_w) = \frac{k}{x}(T_w - T_b) \tag{2}$$

where, T_b is a water-side temperature of the wall, x the wall thickness and k the thermal conductivity.

(c) Transient method
This technique requires measurement of the elapsed time to increase the surface temperature of the TLC-coated test specimen from a known initial temperature predetermined value [4] [11] [12]. The rate of heating is recorded by monitoring the colour change patterns of the TLC with respect to time. If the specimen is made from a material of low thermal diffusity and chosen to be sufficiently thick, then the heat transfer process can be considered to be one-dimensional (1-D) in a semi-infinite block. Numerical and analytical techniques can be used to solve the 1-D transient conduction equation. The relationship between wall surface temperature, T, and heat transfer coefficient, h, for the semi-infinite case is,

$$\frac{T - T_i}{T_a - T_i} = 1 - e^{\beta^2}\,\text{erfc}\,(\beta); \quad \beta = h\left(\frac{t}{\rho c k}\right)^{0.5} \tag{3}$$

where, ρ, c and k are the model density, specific heat and thermal conductivity. T_i and T_a are the initial wall and gas temperatures and t is time from initiation of the flow, Baughn et al. [4] and Jones et al. [12].

(d) Shear stress measurements
TLC's can also indicate shear stress and their use in neat (unencapsulated) form in this mode and gives transition data. It was first investigated at NASA, Moffat [14], and a quantitative measurement method for skin friction was invented later by Bonnett et al. [5]. They observed that if a material in the focal-conic texture on a given surface is suddenly subjected to a steady air flow, then the time for the material to align into grandjean texture is a unique function of the shear stress. This time can be easily measured as it corresponds to the time for the surface to change from a colourless state. Thus, a robust technique independent of viewing angle or illumination became available. In this last case transition was readily detected, Bonnett et al. [5].

(e) Temperature and flow visualisation in fluids
Liquid crystals have been used to make visible the temperature and velocity fields in fluids as well as air. Temperatures have been visualised using the materials in the unsealed (neat) and micro-encapsulated forms as both tracer particles in flow fluid studies and as surface coatings, Hiller et al. [10], Moffat [14], Parsley [15] and Stasiek et al. [17].

5
Application experiments

In order to demonstrate the feasibility of TLC techniques in practical heat transfer contexts the author has performed several experiments. *The first set* was carried out to investigate temperature and heat transfer coefficient distributions on a cooled surface heated by an air flow and disturbed by a number of complex geometrical configurations, namely,

i. Cylinders (both single and double) and a square section column
ii. Square roughness elements and rib-roughened channel
iii. Crossed-corrugated and corrugated-undulated elements as used in rotary heat exchangers (regenerators) for fossil-fuelled power stations.

In the second set of experiments flow structures and temperature distribution in rectangular cavity were visualised using photographic records of the motion of tracer particles illuminated by a sheet of white light. Unsealed TLC's were used to make visible the temperature and velocity fields in a glycerol-filled cavity, which could be angled from horizontal through inclined to vertical.

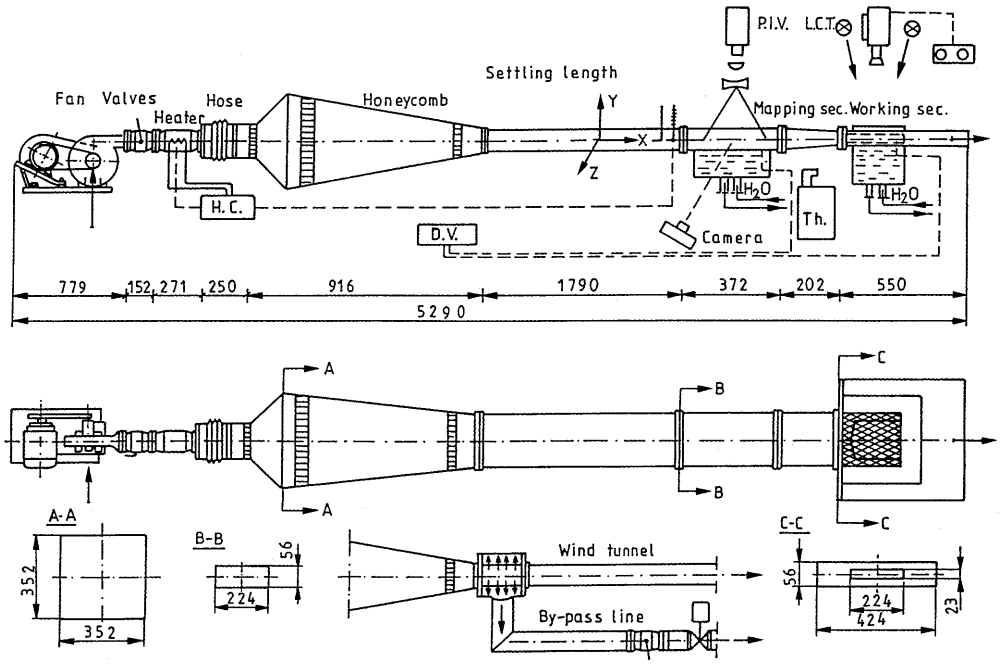

Fig. 7. Open low-speed wind tunnel

5.1
Design and construction of the wind tunnel

The experimental study was carried out using an open low-speed wind tunnel, Fig. 7, consisting of entrance section with fan and heaters, large settling chambers with diffusing screen and honeycomb, and then mapping and working sections Fig. 8 and Fig. 9. Air is drawn through the tunnel using a fan able to give Reynolds numbers of between 500 and 50 000 in the mapping and working sections. The working air temperature in the rig range between 25°C to 65°C produced by the heater positioned just down stream of the inlet. The major construction material of the wind tunnel is perspex. Local and mean velocity are measured using conventional Pitot tubes and DISA hot-wires velocity probe. The wind tunnel is instrumented with copper-constantan (Type T) thermocouples and resistance thermometers so that the surface, water bath and air temperatures can be measured and controlled by a Variac control system. The alternative effects of constant wall temperature and constant heat flux boundary conditions are obtained using a water bath, while the temperature can be controlled with a thermostat capable of establishing and maintaining temperature to within ± 0.01°C accuracy. Photographs are taken using a standard camera, RGB video-camera and true-colour image processing system.

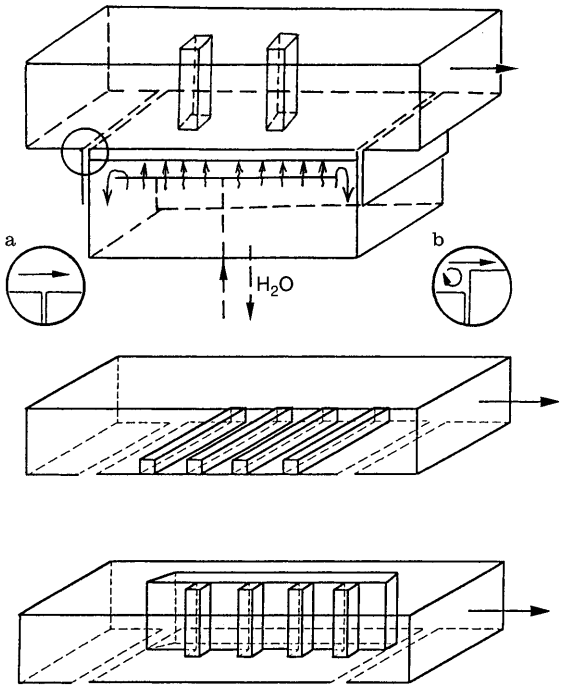

Fig. 8. Mapping section geometry with double a square section column, square roughness elements and rib-roughened channel

5.2
Flow visualisation in a rectangular cavity

Natural convection phenomena in rectangular cavities with differentially heated walls have received considerable attention due to their many applications in energy-sensitive designs such as building systems with cavity walls and air gaps in unventilated spaces, double glazing, solar collectors and furnaces. There are numerous other examples. The thermal convective flow in this study was generated in a rectangular cavity of 180 mm long, 60 mm wide and 30 mm high, Fig. 10. The cavity had isothermal hot and

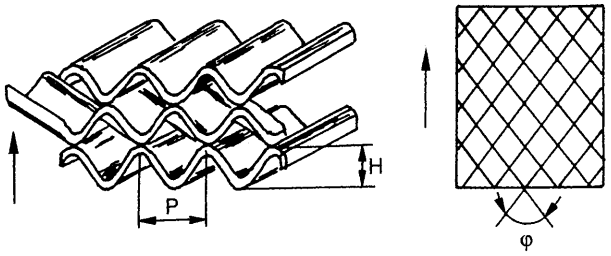

Fig. 9. A general view of a cross-corrugated heat transfer element

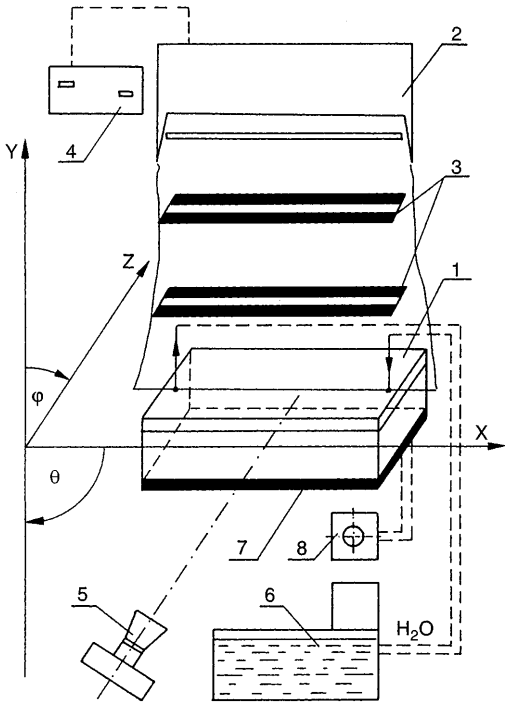

Fig. 10. Schematic diagram of rectangular cavity facility. *1* Cavity, *2* Power flash lamp, *3* Light slots, *4* Programmable generator trigger, *5* Camera, *6* Water bath, *7* 30W blanket heater, *8* Transformer

cold walls and was made from 8 mm perspex (apart from the lower copper plate). The angle of the inclination of the cavity was varied from the horizontal to the vertical for two different planes. The photographs were made perpendicular to the line of the illumination and were taken with 35 mm SLR camera with 90 mm lens.

The set-up is illuminated using a 800 W Xenon flash lamp collimated by a cylindrical lens and two slots to form a slit which may be adjusted over 2–3 mm in width. The flash lamp is triggered by programmable impulse generator at a prescribed time sequence. Usually four to twelve flashes are used to take one colour photograph. The time interval between flashes varied from one to several seconds. To obtain information about the direction of the flow the last flash of a series has been released at half of the prescribed time interval, Hiller et al. [10]. Thermochromic liquid crystals were used to make visible the temperature and velocity fields in the glycerol-filled cavity. The glycerol, liquid-crystal mixture was prepared by dissolving unencapsulated chiral-nematic materials in ether and then spraying the mixture into the air above a free surface of glycerol. The ether evaporated in mid-air, leaving small drops of liquid crystal material which fell into the glycerol forming an "almost monodispersed" suspension of particles approximately 50–80 microns in diameter. The concentration was kept below 0.03% by weight.

In the present experiments interest centred on the shape of the isotherms (not in their absolute temperature values) and on the possibility of applying true-colour image processing system for general observations of three-dimensional structures of heat and fluid flow in an enclosure.

5.3
Mapping heat transfer coefficient distributions

The heat transfer coefficient is a defined quantity, calculated from the surface heat flux and the difference between the surface temperature and some agreed reference temperature. This is usually the far field temperature, the mixed mean temperature or the adiabatic surface temperature. Liquid crystals can be used to determine the distribution of the surface temperature, and if the surface heat flux can be found, this allows evaluation of the heat transfer coefficient or the Nusselt number.

The alternative effects of constant wall temperature and constant heat flux boundary conditions are obtained using

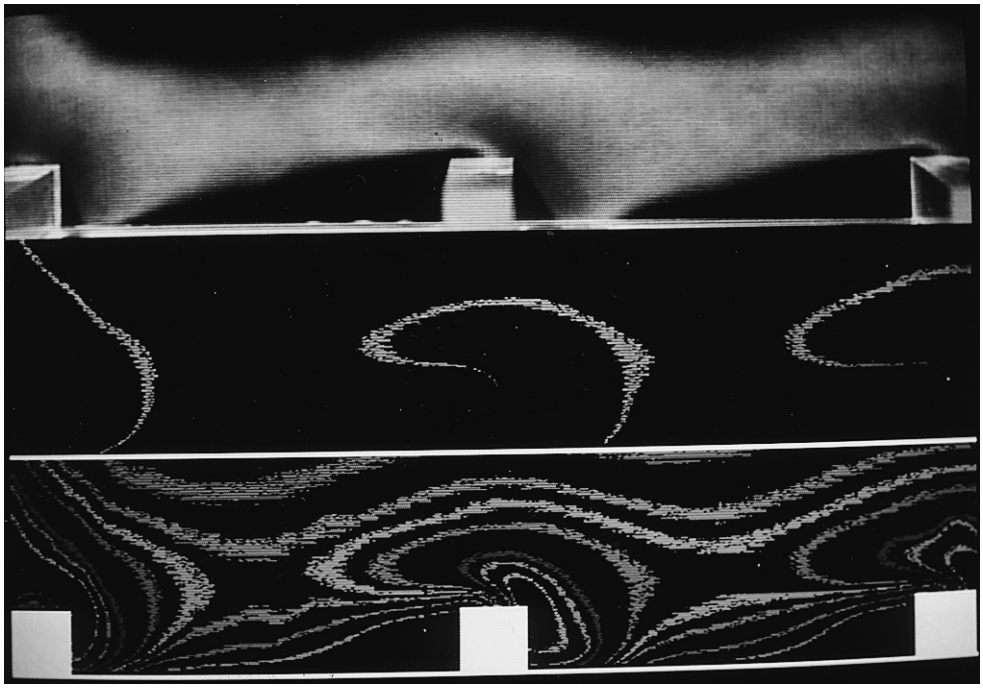

Fig. 11. Image processing steps: true-colour image of the test section under given flow and heating conditions (top), selection of the yellow-green colour band corresponding to a given Nu number value (middle), false colour image corresponding to the superposition of a number of lines at constant Nu number (bottom)

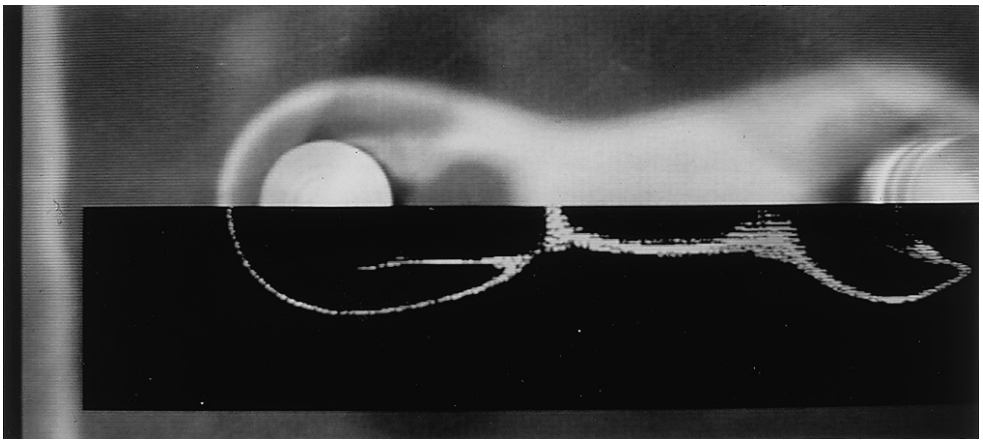

Fig. 12. Comparison between the image from RGB camera and the segmented monochrome 32.1 °C line for the double cylinders column at Re = 2.0 10^4

a water bath. Photographs are taken using a RGB video-camera and a true-colour image processing technique. Usually several isotherms (each corresponding to a different heat flux) are taken by RGB video-camera to record the local Nusselt contours under an oblique Reynolds number. The locations of each isotherm and colour (adjusted to each Nusselt number) are digitized following a projection of the false colour image on a digitizing image respectively (this particular method can be called "Image Combination Technique" ICT). Figure 11 shows photographs of the colour distribution of the liquid crystal layer around square section column (top photo), image of the computer display after segmentation processing (Hue: 45–55) (middle photo) and false colour image processing (ICT) respectively on bottom photo.

The colour image from the RGB camera and the segmentation monochrome line showing the 32.1°C isotherm for the double cylinders column at Re = 2.0 10^4 are presented together in Fig. 12. The image in Fig. 13 shows Nusselt number contours around double cylinders column processed by the ICT. Also (as mentioned above) liquid crystal thermography has been applied to the study of heat transfer by forced convection from a square roughness elements and rib-roughened channel. A sample of the results for these studies is shown in Figs. 15, 16 and 17. In these experiments a square element mounted horizontal

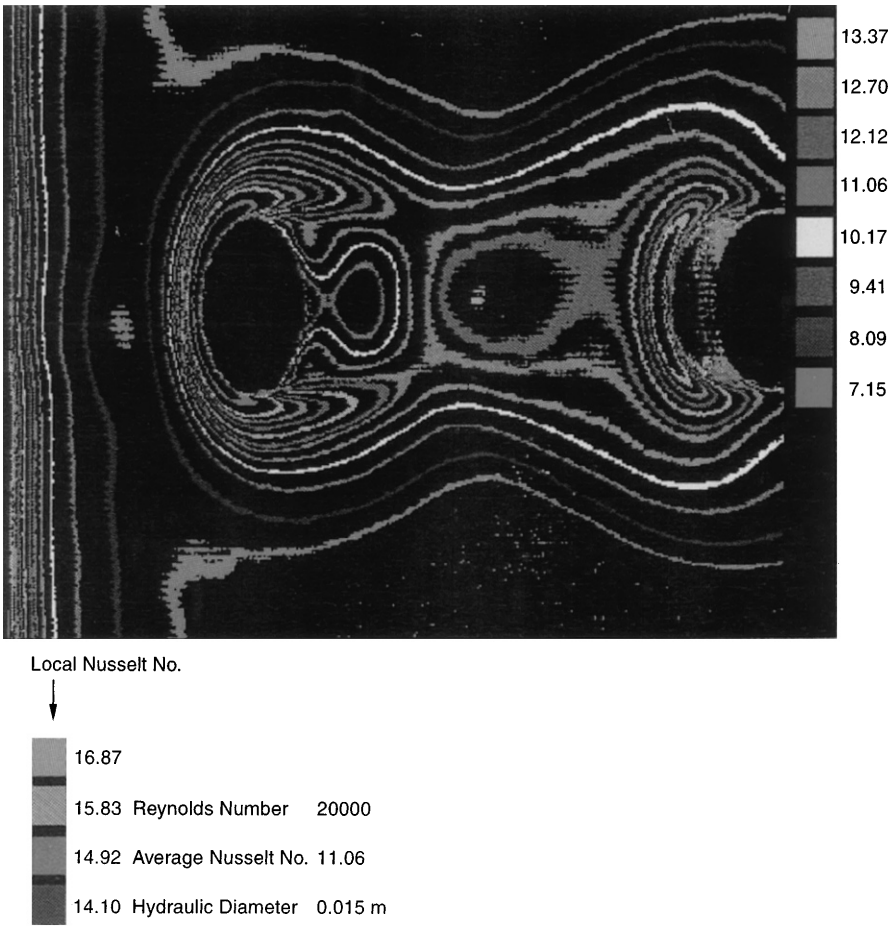

Fig. 13. Colour-scale representation of Nusselt number distribution around double cylinders column processed by image combination techniques

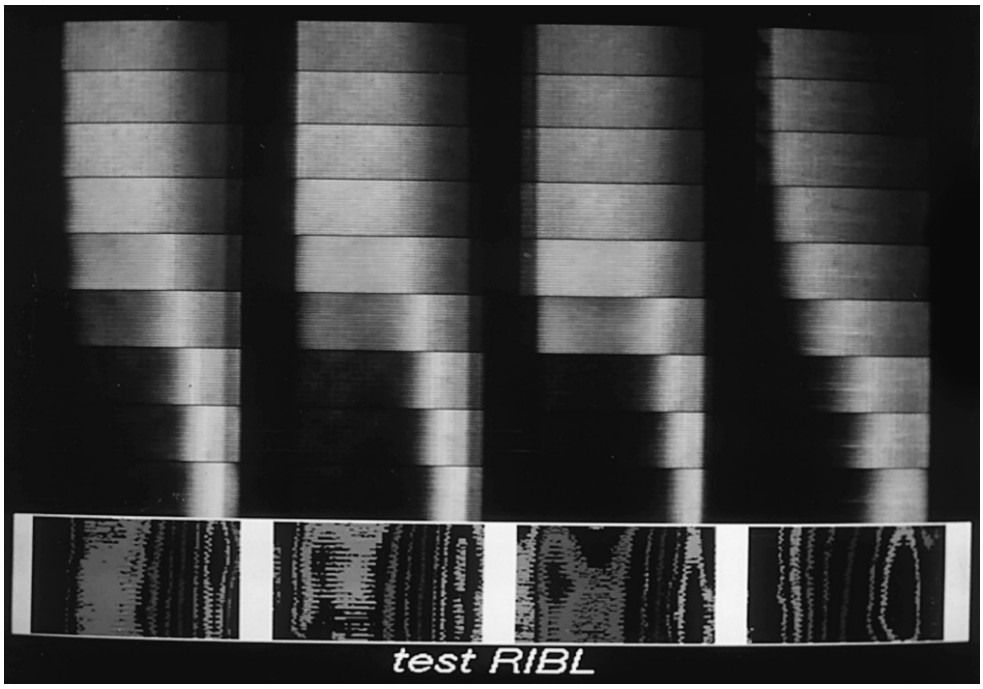

Fig. 14. TLC true-colour images for nine experiments (from top) at fixed Re and different T_a. Bottom figure shows processed image in which the yellow-green colour (isotherm at $T_w = 32.1\,^{\circ}\mathrm{C}$) has been extracted from true-colour images

and normal to the heated flat plate was employed as promotor of turbulence [19][23]. Recording the colour pattern by a RGB video-camera and converting the stored image to the HSI domain allows one to reconstruct the isotherm lines in the new colour scale (ICT) selected arbitrarily for better understanding and visualization of heat transfer and fluid motion. The first investigated geometry consisted of a plane heated wall with square ribs attached at regular intervals – the rib to height ratio was 7.2 for all experiments, Fig. 14. In Fig. 15 the Nusselt number distribution along the wall is reported and compared with interferometric data at the same Re number (between fourth and fifth ribs only). The profile obtained by LC analysis exceeds the interferometric results by 10–25 per cent. It should be pointed out that the geometric parameters (height and width of the channel) as well as thermal boundary conditions were not exactly the same in the two different set of experiments. In spite of this, the agreement is rather satisfactory and demonstrates the suitability of both tech-

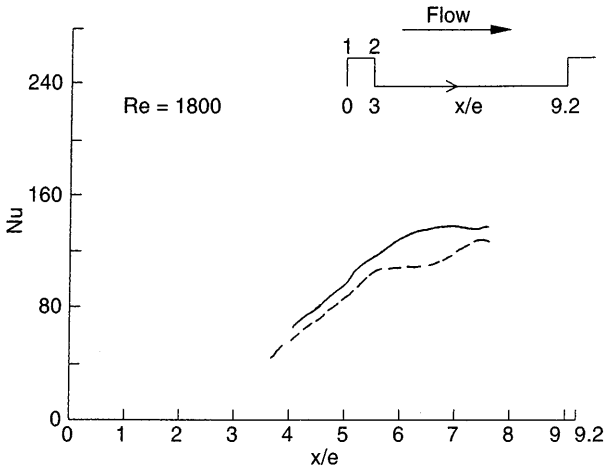

Fig. 15. Nusselt number distribution in the inter-rib region from liquid crystal data in comparison with interferometric data (Re = $1.8\ 10^4$) Continuous line: liquid crystals, dashed line: interferometry

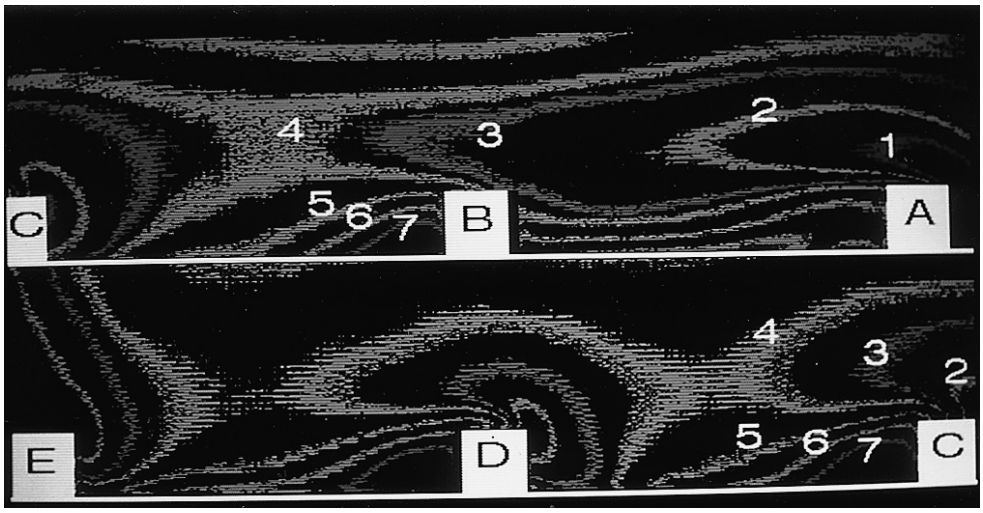

Fig. 16. Colour scale representation of Nusselt number distribution around rib-roughened channel at Re = $1.0\ 10^4$ (1-Nu = 131, 2-Nu = 112, 3-Nu = 93, 4-Nu = 8, 5-Nu = 72, 6-Nu = 61, 7-Nu = 52)

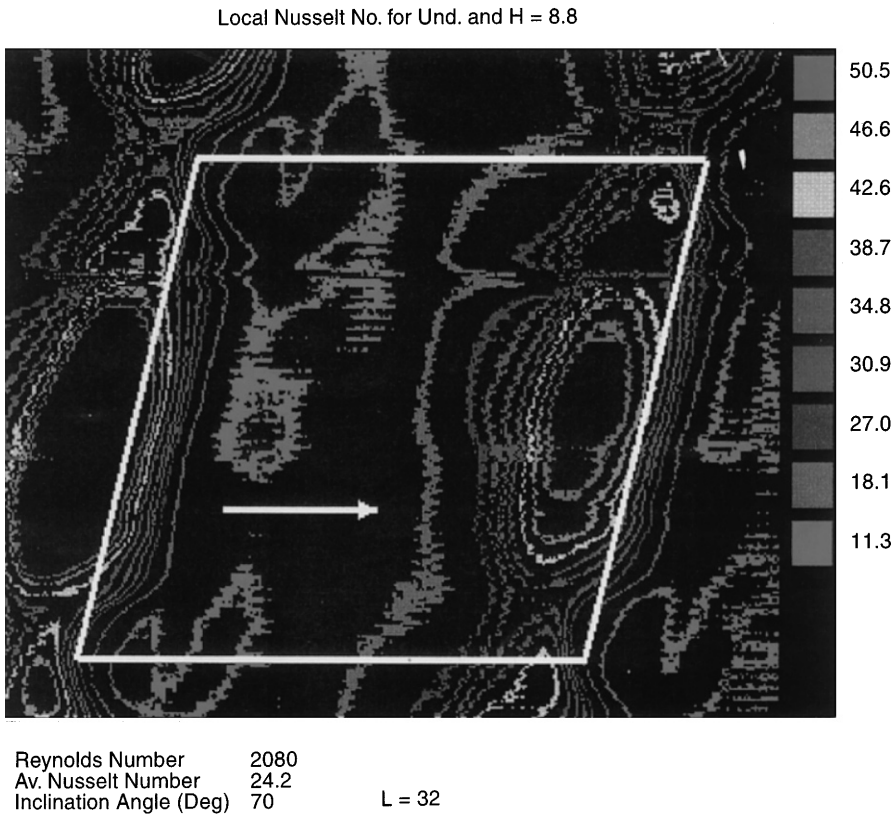

Fig. 17. False colour image of local Nusselt number contours over a central diamond of the undulated plate of corrugated-undulated geometry ($\phi 70^\circ$, Re = 2080, H = 8.8 mm, L = 32 mm)

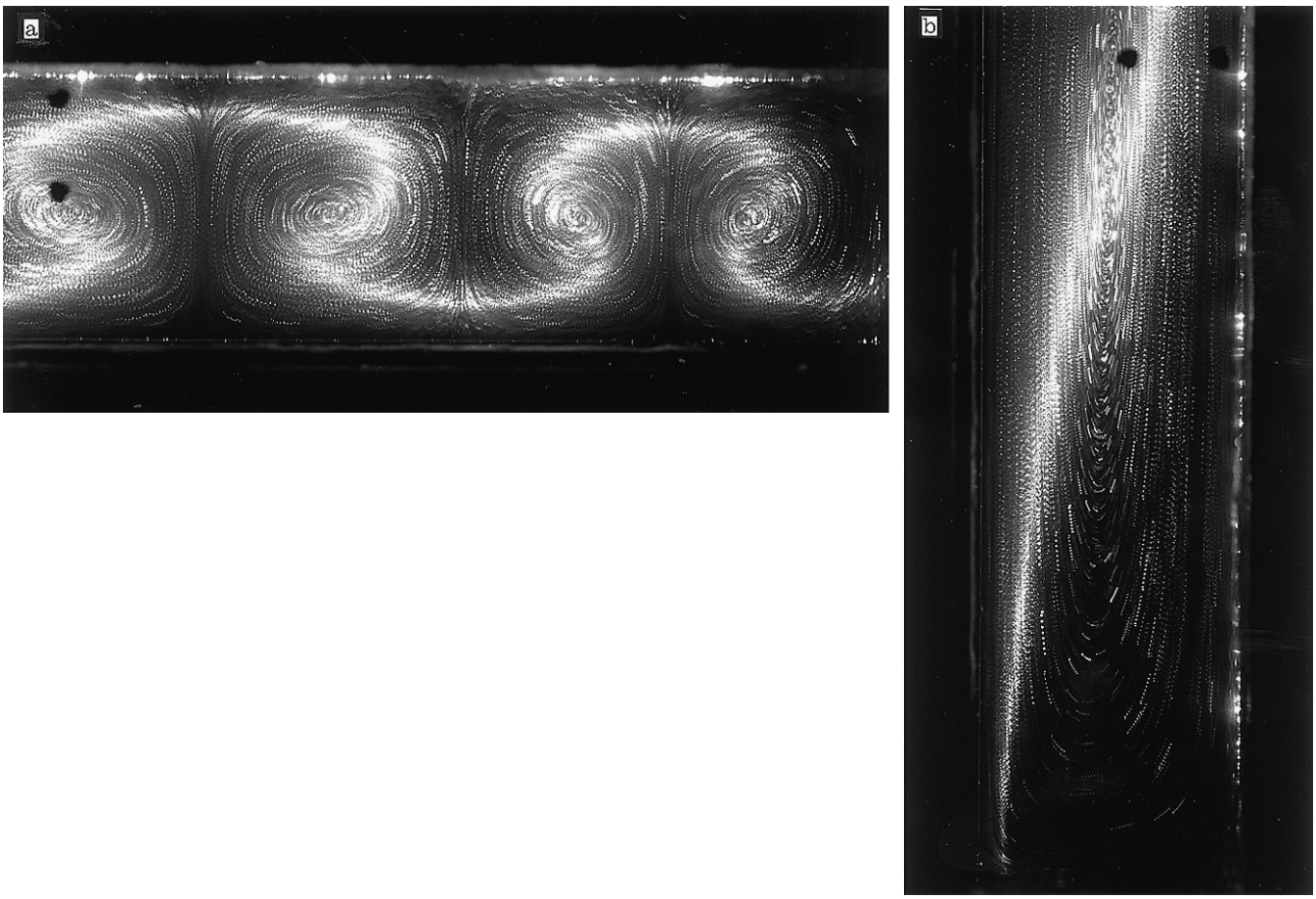

Fig. 18a,b. Temperature and velocity visualisation in glycerol-filled cavity under free convection using chiral-nematic liquid crystal (Re = 1.2 10^4, Pr = 12.5 10^3) **a** horizontal position and **b** vertical position

niques to gain quantitative information on heat transfer distribution in roughened surfaces.

Forced convection heat transfer in rib-roughened channels can be encountered in engineering problems which are extremely diverse. Applications include fuel rods of gas cooled nuclear reactors, inside cavities of turbine blades, internal surfaces of pipes used in heat exchangers, arrays of printed circuit boards, and the surface of solar collectors. As is well known, the use of repeated ribs causes a break up of the laminar sublayer and creates local wall turbulence due to flow separation and reattachment between ribs, which greatly enhances the heat transfer.

A large number of experimental and numerical studies dealing with rib-roughened heat transfer channels have been performed in recent years. Despite this, the present investigation which has been carried on by G. Tanda et al. [21], is apparently the first in which rib-roughened surface is not itself the heat transfer surface but only acts as a vortex generator to increase flow turbulence in the channel. It is well known that an obstacle, mounted normal to a flat plate cooled by forced convection, can increase heat transfer from the plate [23]. In fact the formation of complex secondary flows downstream of the obstacle increases levels of turbulence and mixing, leading to local heat transfer enhancement. An example of the colour-scale representation of local Nusselt number distribution around rib-roughened channel at Re = 1.0 10^4 is presented in Fig. 16. Also Fig. 17 shows a false colour image of local Nusselt number contours over a central diamond of the corrugated-undulated heat exchanger surfaces. The cross corrugated and corrugated-undulated surfaces are frequently employed to increase heat transfer coefficient for high heat flux applications. Improvements in their flow and thermal characteristics does not require any demonstrations and would substantially reduce fuel and production costs. These considerations led to the execution of a comprehensive experimental and analytical investigation at City University supported by PowerGen U.K. [19]. The measuring technique comprising the use of LC flexible sheets and true-colour processing may also be used for a great variety of applications and should be of considerable use in improving the design of all types of compact heat exchanger.

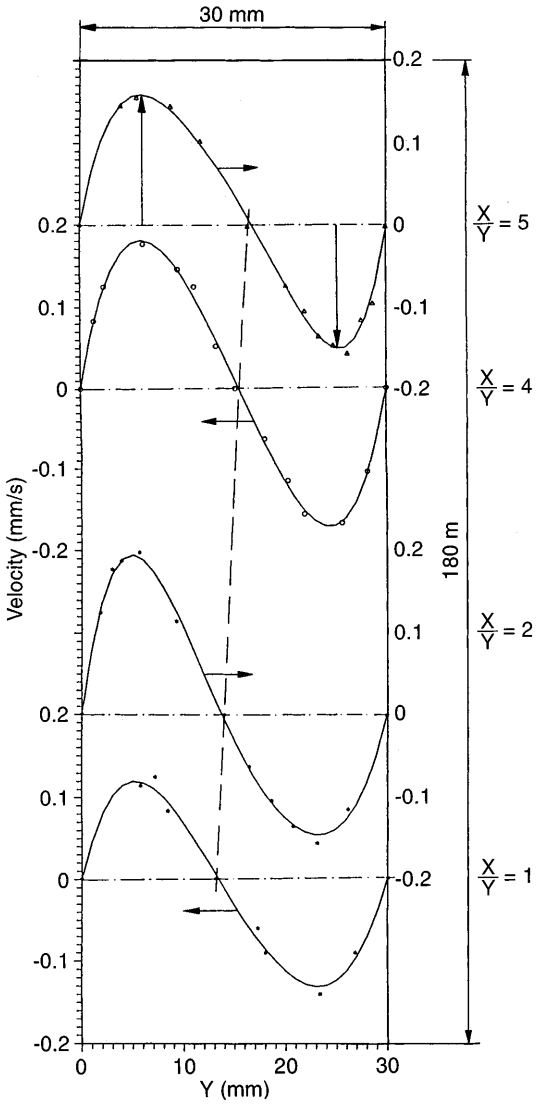

Fig. 19. Vertical velocity profiles at different heights in vertical position of cavity; Ra = 1.2 10^4 and Pr = 12.5 10^3

5.4
Natural convection in a rectangular cavity

In the second set of experiments (Glycerol-filled Cavity) a temperature gradient of 10 K (T_h = 297.6 K, T_c = 287.6 K) so as to obtain desired Rayleigh (Ra = 1.2 10^4), and Prandtl (Pr = 12.5 10^3) numbers and flow conditions in the particular cavity. Figure 18 shows image for the mid-plane of the half cavity taken for the horizontal and vertical position. In this particular experiment 8 flashes at a time interval of 6 seconds were used to take one photograph. The displacements of the tracer particles, as recorded on the photographs, enable information to be obtained about the velocity field in the cavity. This information is, of course, limited to components lying in the plane of observation. An example of the vertical profiles in the mid-plane at various cross sections of the cavity is given in Fig. 19. The isotherm presented in Fig. 20 is a line (white) of constant hue range bands for a picture taken under flow resulting from the vertical configuration of the cavity. This was obtained by taking a photo image using RGB video-camera and then converting the RGB image to a HSI image. This may be used to map isothermal contours, as hue has a direct relationship with temperature that can be found by calibration.

6
Conclusions

A new experimental technique, in this case true-colour image processing of liquid crystal patterns, allows new approaches to old problems and at the same time opens up new areas of research. Image processed data makes available quantitative, full-field information about the distribution of temperature and heat transfer coefficient which will undoubtedly encourage the study of situations which have been, until now, too complex to consider. The measuring technique comprising the use of LC flexible

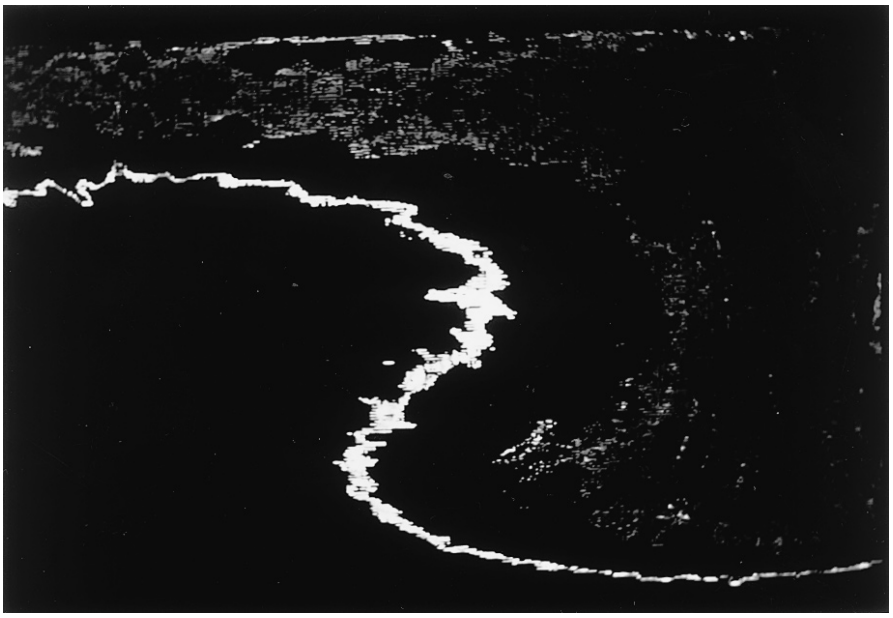

Fig. 20. Segmentation transform of the cavity image shown white isoline for Hue: 100–120

sheets and true-colour processing may also be used for a great variety of applications and should be of considerable use in improving the design of all types of rotary and compact heat exchanger. Also computer aided analysis of colour images of unsealed TLC-tracers is a promising investigative method of three-dimensional flow structure and temperature visualisation in convective flow.

References

1. **Akino, N.; Kunugi, T.; Ichimiya, K.; Mitsushiro, K.; Ueda, M.:** Improved liquid crystal thermometry excluding human colour sensation. ASME J.Heat Transfer 111 (1989) 558–565
2. **Akino, N.; Kunugi, T.; Shiina, Y.; Ichimiya, K.; Kurosawa, A.:** Fundamental study on visualization of temperature fields using thermosensitive liquid crystals. In: Reznicek, R. (ed) Flow Visualization V. Hemisphere Publishing Corporation, Washington (1990) 87–92
3. **Ashforth-Frost, S.; Wang, L.S.; Jambunathan, K.; Graham, D.P.; Rhine, J.M.:** Application of image processing to liquid crystal thermography. Proceedings of the First I.Mech.E. Seminar on Optical Methods and Data Processing in Heat and Fluid Flow. City University, London (1992) 121–126
4. **Baughn, J.W.; Yan, X.:** Liquid crystal methods in experimental heat transfer. Proceedings of 32nd Heat Transfer and Fluid. Mechanics Institute Sacramento, California (1991) 15–40
5. **Bonnett, P.; Jones, T.V.; Donnell, D.G.:** Shear-stress measurement in aerodynamic testing using cholesteric liquid crystals. Liquid Crystal 6 (1989) 271–280
6. **Brown, G.M; Shaw, W.G.:** The mesomorphic state: Liquid crystals. Chem. Rev. 57 (1957) 1049–1157
7. **Cooper, T.E.; Field, R.J.; Meyer, J.F.:** Liquid crystal-thermography and its application to the study of convective heat transfer. ASME J. Heat Transfer 97 (1975) 442–450
8. **Fergason, J.L.:** Liquid crystal in nondestructive testing. Applied Optics 7 (1969) 1729–1737
9. **Goldstein, R.J.; Franchett, M.E.:** Heat transfer from a flat surface to an oblique impinging jet. ASME J. Heat Transfer 110 (1988) 84–90
10. **Hiller, W.J.; Kowalewski, T.A.:** Simultaneous measurement of temperature and velocity fields in thermal convective flows. In: Veret, C. (ed) Flow Visualization IV. Hemisphere Publishing Corporation. Washington (1986) 617–622
11. **Hollingsworth, D.K.; Boehman, A.L.; Smith, E.G.; Moffat, R.J.:** Measurement of temperature and heat transfer coefficient distributions in a complex flow using liquid crystal thermography and true-colour image processing ASME J. Heat Transfer 123 (1989) 35–42
12. **Jones, T.V.; Wang, Z.; Ireland, P.T.:** The use of liquid crystals in aerodynamic and heat transfer experiments. Proceedings of the First I.Mech.E. Seminar on optical methods and Data Processing in Heat and Fluid Flow. City University, London (1992) 51–65
13. **Moffat, R.J.:** Describing the uncertainties in experimental results. Exp. Thermal Fluid Sci. 1 (1988) 3–17
14. **Moffat, R.J.:** Experimental heat transfer. Proceedings 9th Intl. Heat Transfer Conference, Jerusalem, Vol. 1 (1991) 308–310
15. **Parsley, M.:** The use of thermochrome crystals in heat transfer and fluid flow visualization research. FLUCOME'88 Sheffield University U.K. (1988) 216–220
16. **Reinitzer, R.:** Beiträge zur Kenntniss des Cholestrins. Monatschr, Chem. Wien, 9 (1988) 421–441
17. **Stasiek, J.; Collins, M.W.:** The use of liquid crystals and true-colour image processing in heat and fluid flow experiments. Atlas of Visualization Vol. 2. CRC Press, Inc. U.S.A. 1996
18. **Stasiek, J.; Collins, M.W.; Chew, P.E.:** Liquid crystal mapping of local heat transfer in crossed corrugated geometrical elements for air heat exchangers. Proceedings of the EUROTECH-Direct '91-Thermofluids Engineering. I.Mech.E. U.K. (1991)
19. **Stasiek, J. et al.**: Local heat transfer and fluid flow fields in crossed corrugated geometrical elements for rotary heat exchangers Report No. 1 to 13 TFERC, City University, London (1989–1994)
20. **Stephen, M.J.; Straley.:** Physics of Liquid Crystals. Review of Modern Physics 46, No. 4 (1974). 617–704
21. **Tanda, G.; Stasiek, J.; Collins, M.W.:** Application of holographic interferometry and liquid crystal thermography to forced convection heat transfer from a rib-roughened channel. Intl. Conference on Energy and Environment, Shanghai China (1995) 8
22. **Tanda, G.; Ciofalo, M.; Stasiek, J.; Collins, M.W.:** Experimental and numerical study of forced convection heat transfer in a rib-roughened channel. Proceedings of the XIII

UIT National Heat Transfer Conference, Bologna, Italy (1995) 243–254

23. Zhang, X.; Stasiek, J.; Collins, M.W.: Experimental and numerical analysis of convective heat transfer in turbulent channel flow with square and circular columns. Exp. Thermal Fluid Sci. 10 (1995) 229–237

24. DATA TRANSLATION Ltd: Image Processing Handbook 1991

25. MERC Ltd., Poole, Dorset, U.K. Thermochromic Liquid Crystals – Manufacturer's catalogue (1994)

26. B & H LIQUID CRYSTAL DEVICES Ltd, London 1992